International Journal of Industrial Ergonomics 41 (2011) 494–508

Contents lists available at ScienceDirect

International Journal of Industrial Ergonomics

journal homepage: www.elsevier.com/locate/ergon

Tuned vibration absorber for suppression of hand-arm vibration in electric grass trimmer

Ko Ying Hao, Lee Xin Mei, Zaidi Mohd Ripin*

The Vibration Lab©, School of Mechanical and Aerospace Engineering, Engineering Campus, Universiti Sains Malaysia, 14300 Nibong Tebal SPS, Pulau Pinang, Malaysia

ARTICLE INFO

Article history:
Received 17 August 2010
Received in revised form
6 May 2011
Accepted 27 May 2011
Available online 13 July 2011

Keywords:
Hand-arm vibration
Hand tools
Tuned vibration absorber
Subjective rating

ABSTRACT

Prolonged use of electric grass trimmer exposes the user to the risk of hand-arm vibration syndrome. A simple approach for the suppression of hand-arm vibration in electric grass trimmer is presented. The proposed system is a tuned vibration absorber (TVA). Modal analysis and operating deflection shape analysis of the electric grass trimmer were carried out and a TVA was designed and fabricated for testing. The results indicated that minimum vibration level was related to the position of the TVA on the shaft of electric grass trimmer. The TVA was found to have best performance with 95% reduction on the acceleration level at position 0.025L. The results from modal analysis and operating deflection shape revealed that the presence of TVA has successfully reduced the large deformations of the handle where the node was shifted nearer to the handle location. The effect of TVA was also evaluated during field test involving grass trimming operation and subjective rating. The results indicated that average reduction of frequency-weighted rms acceleration in the $Z_{h\text{-}}$ axis was 84% and 72% in $X_{h\text{-}}$ axis for the cutting operation. For the no cutting operation, the reduction is 82% in $Z_{h\text{-}}$ axis and 67% in $X_{h\text{-}}$ axis. The presence of TVA in the electric grass trimmer has amplified the vibration level in $Y_{h\text{-}}$ axis by 19% (no cutting) and 21% (cutting). From the field test, subjective rating of vibration perception consistently rate better for controlled electric grass trimmer.

Relevance to industry: The tuned vibration absorber when installed to the electric grass trimmer attenuated the vibration total value by 67%. This significantly reduces the risk of hand-arm vibration syndrome.

1. Introduction

Grass trimming is usually carried out with the use of petrol engine or electric motor powered trimmer which uses a rotating nylon string that cut the grass. The use of petrol engine is subjected to emission regulation which limits their application. The US Environmental Protection Agency (2010) has adopted new regulations for small engines (operate at or below 19 kW) that are widely used in lawn and garden area. Electric models produce no emissions at the point of use. This factor favours the application of electric grass trimmer for maintenance of grass compound in places where emission is regulated. The electric grass trimmer usually employs an AC electric motor of 400 W with the plastic rotating head coupled directly to the motor. A single nylon string is attached to the rotating head. The single string construction of the electric grass trimmer made it a rotationally unbalanced which resulted in high level of vibration. Under this condition the user is exposed to hand-arm vibration (HAV). Extensive exposure of HAV can lead to a series of vibration induced disorder in the vascular and nonvascular structures in human hand-arm. These disorders are referred to hand-arm vibration syndrome (HAVS) (Mansfield, 2005).

HAVS is classified as an industrial disease and has been affecting innumerable workers. Loriga in 1911 is the first to document the relationship between the exposure of HAV and HAVS (Bylund, 2004). Great efforts have been made by researchers in order to reduce vibration of hand tools and its effect. These included isolation of the hand from the vibrating handle with the use of anti-vibration gloves (Brown, 1990; Muralidhar et al., 1999; Voss, 1996). The effect of anti-vibration gloves to the human–tools interface has been extensively studied, such as the investigation of the vibration isolation characteristic for a gloved hand using a laser-based vibration sensor (Gurram et al., 1994); development of a more reliable method for assessment of effectiveness of anti-vibration glove (Dong et al., 2003); evaluation of the effect of wearing anti-vibration gloves on the grip strength applied to cylindrical handles (Wimer et al., 2010). However, different hand

* Corresponding author.
E-mail address: mezaidi@eng.usm.my (Z.M. Ripin).

0169-8141/$ – see front matter © 2011 Elsevier B.V. All rights reserved.
doi:10.1016/j.ergon.2011.05.005

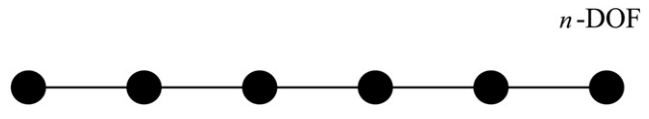

Fig. 1. Electric grass trimmer system represents a *n*-DOF model.

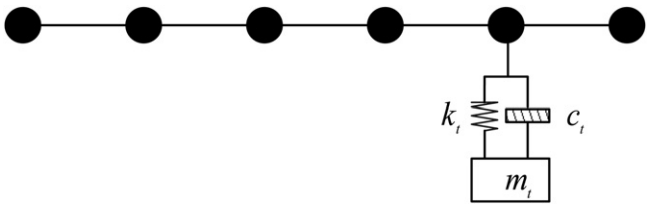

Fig. 2. Modified electric grass trimmer system with TVA attached to the *n*-DOF model.

tools will have different influence on the isolation performance of the anti-vibration glove as it is tool or excitation spectrum specific (Rakheja et al., 2002). In certain cases where the machines have clear handle modules, vibration attenuation can be achieved by the isolation of the tool handle from the vibrating source using vibration isolators (Sam and Kathirvel, 2006; Tewari and Dewangan, 2009). Another feasible technique is to channel the vibration energy to a secondary system by adding a secondary mass-spring-damper to a primary system which is known as tuned vibration absorber (TVA). This will reduce the vibration of the vibrating system thus reducing the handle vibration.

The first invented TVA has no damper. It was useful only in a narrow range of frequencies (Asami et al., 2002). Ormondroyd and Den Hartog (1928) showed that lightly damped TVA is effective for optimum broadband attenuation. By balancing two invariant points in the frequency response, Den Hartog derived the optimum tuning ratio and damping ratio of TVA attached to an undamped single-degree-of-freedom (SDOF) primary system (Rao, 2004). Since this pioneering approach, many TVA optimization work were carried out. Asami et al. (2002) demonstrated an analytical series solution for optimum TVA when attached to damped SDOF system. Ren (2001) designed a variant design of TVA which reported having better vibration suppression performance. Many papers model the primary system as damped SDOF system (Asami et al., 2002; Ren, 2001; Wong and Cheung, 2008). However for practical purposes, the primary structures would always have to be treated as multiple-degrees-of freedom (MDOF) systems or continuous models that have multiple vibration modes and resonant frequencies. In order to deal with the multiple modes vibration, many studies have focused on the concept of TVA mounted on the MDOF system or continuous model (Brennan and Dayou, 2000; Cheung and Wong, 2008; Dayou, 2006; Thompson, 2007; Zuo and Nayfeh, 2004). Ozer and Royston (2005) extended Den Hartog's approach to derive an optimum TVA attached to the undamped MDOF system. Esmailzadeh and Jalili (1998) carried out a study on the determination of optimum tuning and damping ratio of TVA for a structural damped Timoshenko beam model. Dayou (2006) examined the control of kinetic energy of a continuous models using Fixed-point theory. The TVA comes in various design concepts, from the traditional (Den Hartog, 1956) to non-traditional (Ren, 2001; Wong and Cheung, 2008), from SDOF absorber to MDOF absorber (Dayou and Brennan, 2002; Jang and Choi, 2007; Thompson, 2007). One of the well known design concept is the beam like vibration absorber or dual cantilevered mass vibration absorber. This type of absorber consists of a beam with a mass attached on its end. The span of the beam can be varied to adjust the natural frequency of the absorber (Brennan, 2000; Kidner and Brennan, 2002).

In practical application, Strydom et al., (2002) designed a vibration absorbing handle for rock drill. The TVA was tuned so that it coincides with the operating frequency of rock drill. The attenuated handle has reduced the vibration transmissibility by 20%–40%. Lee et al. (2001) developed a damped passive TVA on a cutting tool to suppress vibration in turning operations. Acceleration level of the cutting tools with the presence of a well tuned TVA showed the reduction of acceleration level from 100 g to 30 g. Fasana and Giorcelli (2010) studied the application of the concept of TVA to motorcycle handle. The TVA was tuned to the frequency of maximum discomfort of biker. The attenuation of vibration is positive with the presence of TVA even if not perfectly tuned. Golysheva and Babitsky (2004) showed that vibration attenuation of hand-held percussion machine could be very effective with combination of isolation and absorption principles. By introduce two TVAs (one tuned to fundamental frequency and the other tuned to second harmonic frequency) attached to the isolated handle resulted reduction of the amplitude at fundamental

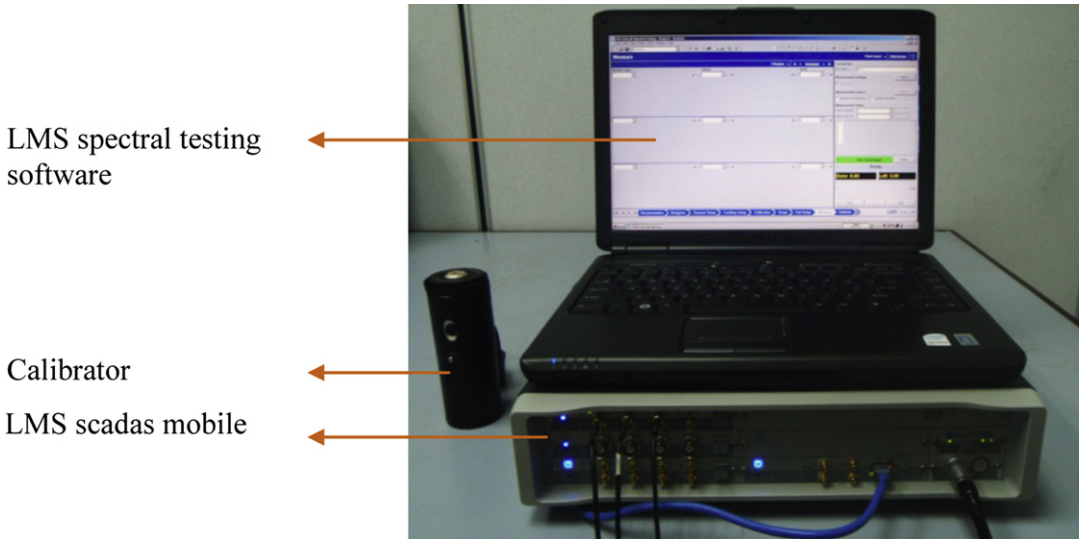

Fig. 3. Test equipments for vibration analysis.

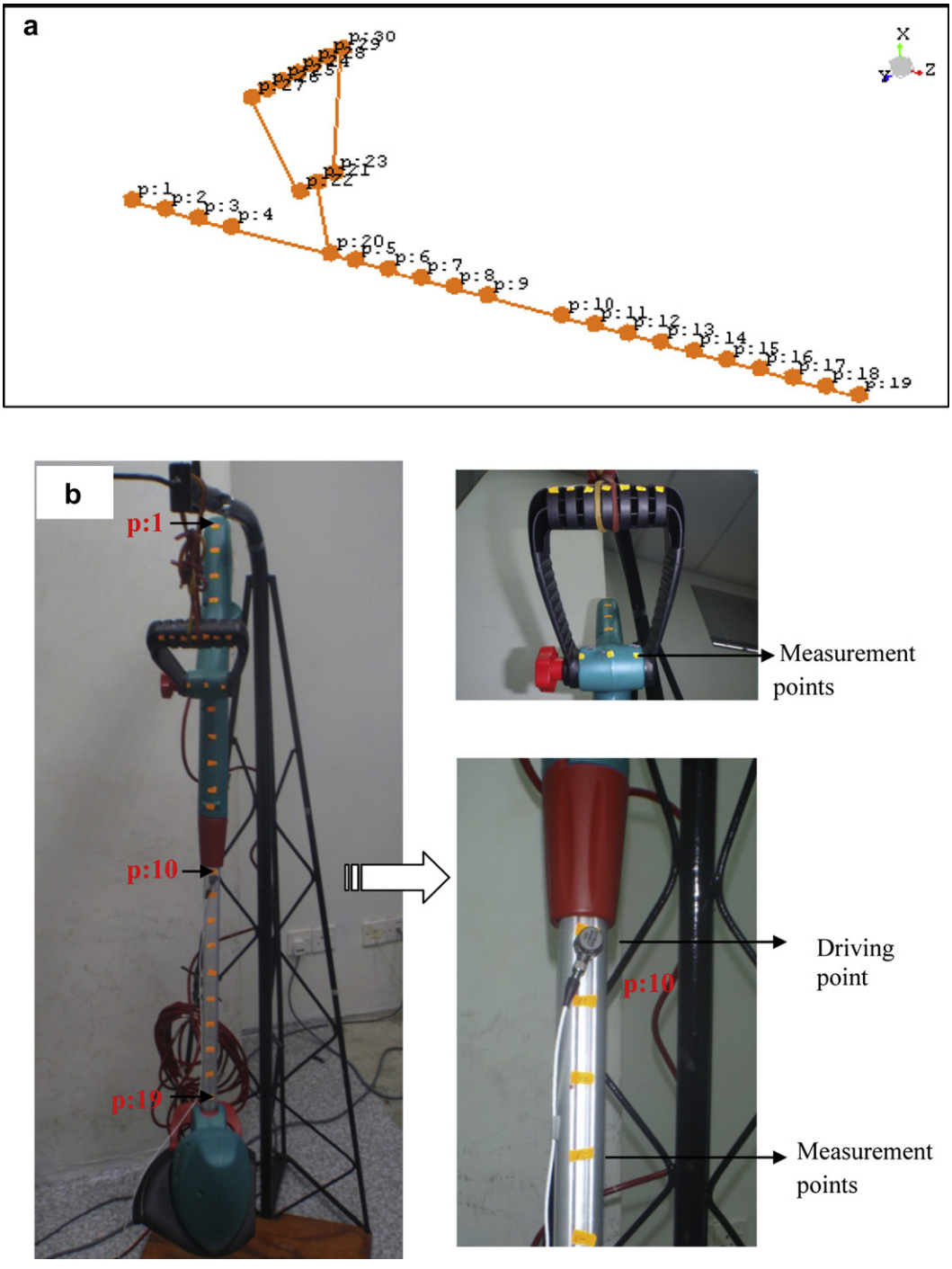

Fig. 4. (a) Geometry model of electric grass trimmer and (b) Measurement points on electric grass trimmer.

frequency and second harmonic frequency by a factor of 62 and 70 respectively. Kadam (2006) attached a vibration absorber at the handle of pneumatic impact hammer and showed the vibration level of handle response reduced in the range of 5–10 dB.

An important parameter in designing TVA for MDOF or continuous system is the location of the absorber location (Petit et al., 2009). This parameter has a large influence on the possibility of vibration reduction. Interestingly, recent studies have shown that the vibration of a location on beam can be made stationary near the resonant frequency by properly choosing the absorber parameters (mass and spring constant) and the attachment location of the absorber (Cha and Pierre, 1999; Cha, 2002; Cha, 2005; Cha and Ren, 2006; Cha and Zhou, 2006; Cha and Chan, 2009; Foda and Bassam, 2006; Wong et al., 2007). These studies showed that, for a machine which can be modelled as a beam, there is the possibility of locating the node at the desired location preferably the handle location for a high reduction of vibration level.

Several studies have confirmed that the levels of vibration on petrol driven grass trimmer are high enough to cause an enhanced level of risk of HAVS (BS EN ISO 11806, 2008; Tudor, 1996) which indicate the need to reduce vibration level of grass trimmer

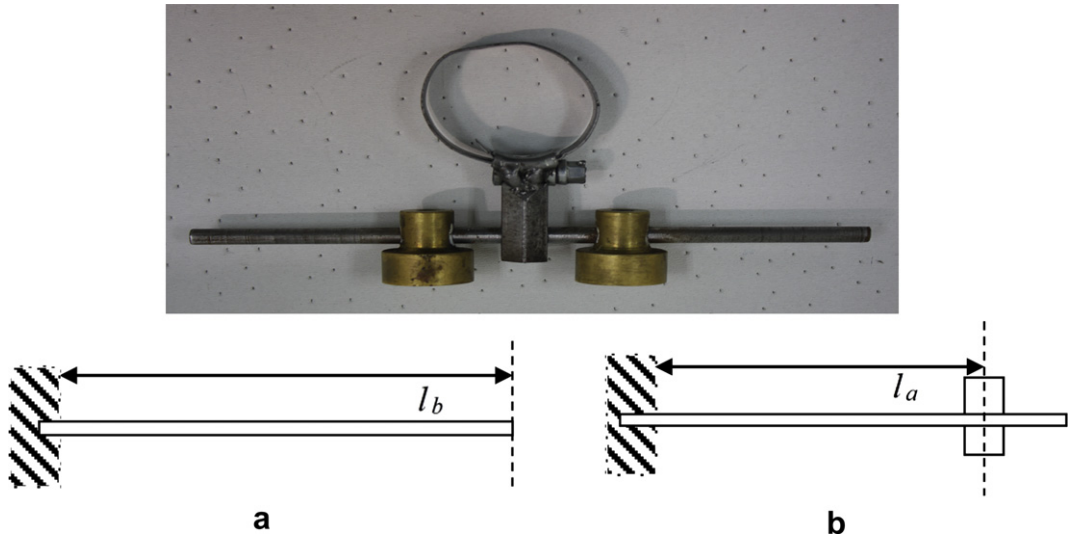

Fig. 5. Design of TVA with dual cantilevered mass.

exposure to the operator. Conventional approaches to reduce the vibration level at the handle of tools, such as the use of vibration isolators, however results in handle with a high mass and low stiffness (Strydom et al., 2002). Another more recent approach to minimize the vibration of grass trimmer was by carefully selecting the optimum parameters of grass trimmer, such as hand-handle position, engine operating speed, sway angle, length of nylon string and the material of handle (Mallick, 2008, 2010). However, it could be difficult for the workers to adopt the suggested optimum parameter in the grass trimming operation.

The state of the art on vibration attenuation on grass trimmer indicated that the level of vibration is still high and dangerous for long term use. This paper presented a research work on the applicability of TVA to suppress vibration of electric grass trimmer. The effect of TVA is firstly obtained using structural modification (SM) based on experimental modal analysis and the results are later compared with the experimental results. The TVA is designed and built in order to evaluate its performance in practice. To ensure that the solution suggested being practical, the measured frequency-weighted rms acceleration and operator judgement in terms of vibration perception during the field test operation was also performed.

2. Theoretical consideration: effect of attaching a TVA to grass trimmer

Attaching a TVA on the shaft of electric grass trimmer will invariably change the dynamic behaviour of the structure. The changes in the structural behaviour (natural frequencies, mode shapes and frequency response) can be identified by SM procedure (Sestieri, 2000). Depending on the data used in the analysis, SM procedure can be employed from a modal model or finite-element (FE) model of the structure, or directly from frequency response function (FRF) of experimental modal analysis (Jimin, 2001).

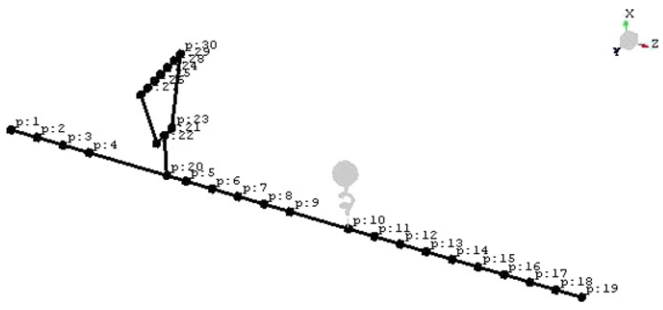

Fig. 6. A simulated TVA attached to the shaft of electric grass trimmer.

2.1. Grass trimmer modal model

The dynamics of the grass trimmer system is assumed to be linear and discretized for n degrees-of-freedom (DOF) (Fig. 1).

The equation of motion of the system in free vibration is expressed as:

$$[\mathrm{M}]\left\{\ddot{x}\right\} + [\mathrm{C}]\{\dot{x}\} + [\mathrm{K}]\{x\} = \{0\} \tag{1}$$

where the matrices M, C and K are the mass, stiffness, and damping matrices of the structure. $\{x\}$ and $\{f\}$ are the displacement and force vector.

Using the standard coordinate transformation, $\{x\} = \Phi\{q\}$ and pre-multiply byΦ^T, the previous equation becomes:

$$\mathrm{I}\left\{\ddot{q}\right\} + \Xi\{\dot{q}\} + \Lambda\{q\} = \{0\} \tag{2}$$

where eigenvectors(modes)$\Phi = [\phi_1 \quad \cdots \quad \phi_n]$, $\Xi = \alpha I + \beta\Lambda$, and eigenvalue Λ,

$$\Lambda = \begin{bmatrix} \omega_1^2 & & \\ & \ddots & \\ & & \omega_n^2 \end{bmatrix} \tag{3}$$

The eigenvectors and the eigenvalues in this work are derived from the experimental modal analysis.

2.2. Tuned vibration absorber modification

Suppose a TVA is attached to the n-DOF grass trimmer model (Fig. 2). The TVA is a SDOF system consisting of a rigid mass m_t, spring k_t and a dashpot c_t. Adding a TVA to the n -DOF model will modify the system and change the parameter matrices of the structure and Eq. (1) represents the equation of motion of the modified system:

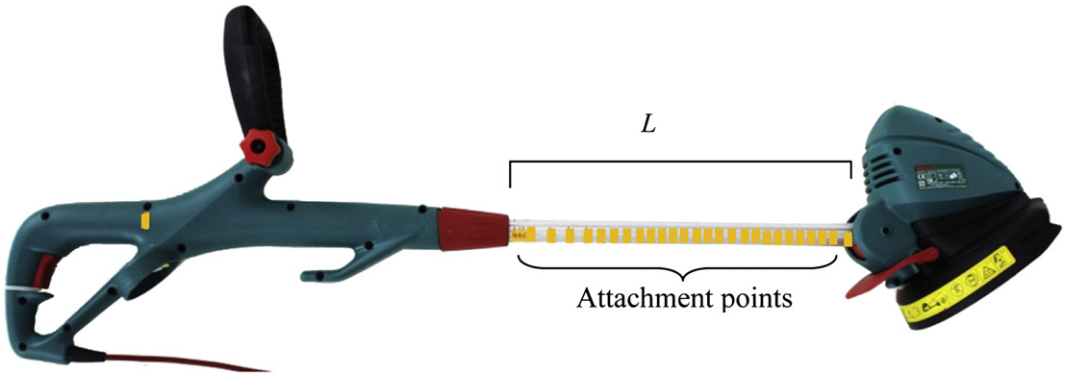

Fig. 7. Attachment points of TVA along the shaft of electric grass trimmer.

$$[M+\Delta M]\{\ddot{x}\}+[C+\Delta C]\{\dot{x}\}+[K+\Delta K]\{x\}=\{0\} \quad (4)$$

where ΔM, ΔC and ΔK are the modified mass, stiffness and damping matrices.

Using again the coordinate transformation $\{x\}=\Phi\{q\}$ and pre-multiply byΦ^T, Eq. (4) becomes,

$$\left(I+\Phi^T\Delta M\Phi\right)\{\ddot{q}\}+\left(\Xi+\Phi^T\Delta C\Phi\right)\{\dot{q}\}+\left(\Lambda+\Phi^T\Delta K\Phi\right)\{q\}=\{0\} \quad (5)$$

where

$$\begin{array}{lcl} I+\Phi^T\Delta M\Phi & = & \tilde{M} \\ \Xi+\Phi^T\Delta C\Phi & = & \tilde{C} \\ \Lambda+\Phi^T\Delta K\Phi & = & \tilde{K} \end{array} \quad (6)$$

This equation established a new equation of motion with new mass $\tilde{M}$, damping $\tilde{C}$ and stiffness $\tilde{K}$ matrices, which can be defined using the modal parameters (natural frequencies, mode shapes, damping) of the original structure from experimental modal analysis, as well as the matrices ΔM, ΔC and ΔK are known. It is worthwhile to point out that the computation of modified modal parameters though Eq. (5) does not require knowledge of the matricesM, C and K of the original structure (Ewins, 1984).

2.3. Prediction of the modified frequency response function

Vibration problem can be identified from FRF, which represents the relationship between the input and the output of a system. FRF plays an important parameter in SM technique and can be directly obtained from experiment. The FRF could be in the form of receptance, mobility, or inertance. The dynamic stiffness matrix $s(\omega)$ is defined as the inverse of the FRF matrix:

$$[s(\omega)]=[H(\omega)]^{-1} \quad (7)$$

The dynamic stiffness matrix of the modified structure can be identified by formulating a modification matrix $[\Delta s(\omega)]$ and adding the same to $[s(\omega)]$. The FRF of the modified structure $[H_m(\omega)]$ can then be predicted as:

$$[H_m(\omega)]=[[s(\omega)]+[\Delta s(\omega)]]^{-1} \quad (8)$$

Table 1
Physical characteristics of the operators participated in the field test.

Attribute	Mean	Standard deviation	Range
Age (years)	28.1	4.04	25–38
Height (cm)	174.8	7.15	160–184
Weight (kg)	69.5	9.25	58–85

3. Materials and methods

3.1. Grass trimmer description

The electric grass trimmer with a weight of 2.74 kg was used in this study. The basic element of the electric grass trimmer consists of the cutting head, connected by a tubular hollow aluminium square structure on which is fitted the upper plastic casing which houses the handle and the switch controlled by the operator. The tubular hollow aluminium structure has an adjustable collar which allows the operators to adjust the overall length of the trimmer to suit their height.

3.2. Vibration analysis of electric grass trimmer

Vibration analysis is carried out in order to determine the operating frequency of the electric grass trimmer, the vibration level and the dominant axis. Vibration analysis was carried out in accordance with ISO 5349-1, (2001). The instruments used in this measurement are shown in Fig. 3 which include the miniature triaxial accelerometer (Dytran, 3023M20), calibrator (B&K, 4294), FFT analyzer (LMS Scadas Mobile) and post-processing software (LMS Spectral Testing).

The electric grass trimmer was tested under free-running condition. Since the length of nylon string for grass trimmer has some influence on the engine speed (Mallick, 2010), a constant length of nylon string was used throughout the study. The accelerometer is mounted on the front handle near the hand grip location. The data from the accelerometer are stored and analyzed using LMS Spectral Testing. Vibration total values a_{hv} are calculated from the frequency-weighted rms acceleration measured in three orthogonal axes ($X_{h\text{-}}$ $Y_{h\text{-}}$ and $Z_{h\text{-}}$) of the handle according to the definition in ISO 5349-1 (2001). The $Z_{h\text{-}}$ axis is defined as the longitudinal axis from third metacarpal bone towards the distal end of the finger. The $X_{h\text{-}}$ axis is perpendicular with $Z_{h\text{-}}$ axis. The $Y_{h\text{-}}$ axis is perpendicular to $X_{h\text{-}}$ and $Z_{h\text{-}}$ axes and is the direction towards the thumb (ISO 5349-1, 2001).

3.3. Experimental modal analysis

The inherent dynamics characteristics of a structure can be determined from experimental modal analysis (He and Fu, 2001). Frequency response functions (FRFs) of a structure are determined through experimental modal analysis which establishes the relationship between measured output and input as a function of

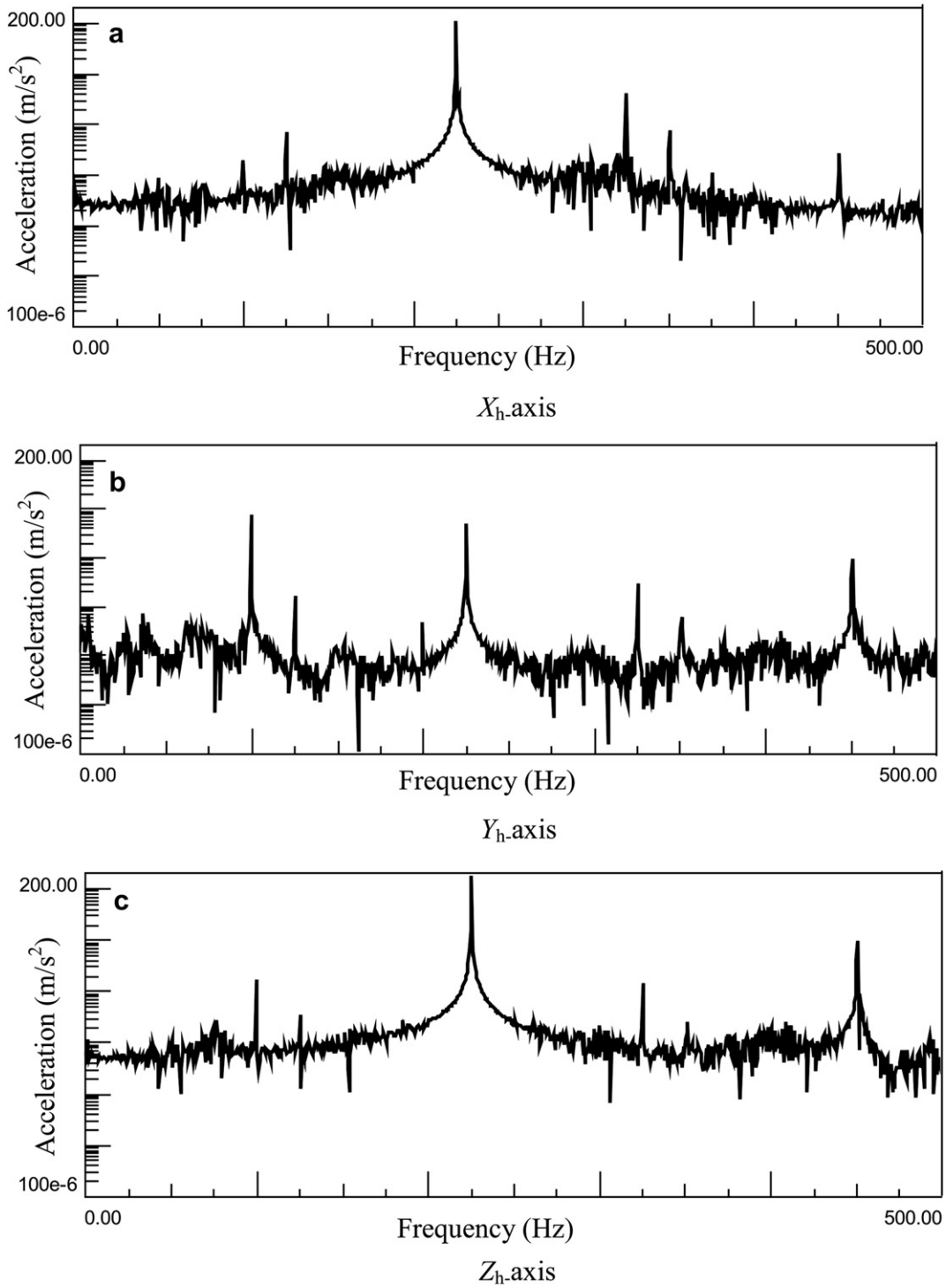

Fig. 8. Acceleration spectra of the electric grass trimmer.

frequency. From these FRFs, the natural frequencies, damping, and mode shapes of a structure can be obtained and can be used to predict the effect of SM. It is an important tool in evaluating and controlling the effect of resonance. Impact testing has become a popular method to perform experimental modal analysis since it is fast, convenient and cost effective (Richardon, 1997).

Fig. 4(a) shows the measurement points on the model of the electric grass trimmer. The experimental modal analysis was carried out with the electric grass trimmer suspended using rubber chords, as shown in Fig. 4(b). This is to stimulate the free–free boundary conditions of structure so that the modal behaviour of the electric grass trimmer can be derived. An impact hammer (Kistler, 9724A5000) fitted with a piezoelectric force transducer was used to excite the electric grass trimmer while a light-weight accelerometer (Dytran, 3055B2 T) was used to measure the vibration response on each measurement point in the X_{h-} axis. The response in Z_{h-} axis was not measured since the axial vibration is small. The handle, in fact, has the minimum vibration level along Y_{h-} axis (from measurement in Section 4.1) which proved that the acceleration in this direction required no further attenuation.

After the accelerometer is calibrated, it was attached on the driving point of the electric grass trimmer, at point 10 (p: 10). Selection of the driving point location is based on the objective in order to excite as many fundamental modes as possible. Excitation and response signals from the test were computed using LMS Scadas Mobile to derive the FRF for each measurement point and the results were post processed and displayed on LMS Impact Testing Rev. 8B software.

3.4. Operational deflection shape (ODS)

In order to study the dynamic behaviour of electric grass trimmer in the real operating condition, ODS analysis was also carried out. Contrary to experimental modal analysis, the measurement of the force acting on the structure are not required, and the ODS depends on the operating parameters of structure (Christof et al., 2010).

ODS can be obtained from the transmissibility measurement by extracting the relative magnitude and phase at the frequency of interest (Schwarz and Richardson, 1999). The frequency range in this case is within 1–1024 Hz, which covers the operating speed of the motor (13200 rpm). Transmissibility measurements are similar with FRF measurements on experimental modal analysis. It is obtained in the same way as FRF measurement, but the response is divided by a reference response instead of the excitation force. The best choice of the reference is the point of maximum response (Christof et al., 2010). In this case, point 19 (p:19) in Fig. 4 is chosen as the reference point. Although, in the ideal ODS analysis, all measurement points are required to be measured simultaneously, due to the limited number of accelerometers and channels, roving method was chosen. A response accelerometer is moved from one measurement point to another during data collection. All response-reference response pair at each measurement point was saved. The ODS post-processing was then carried out using LMS Spectral Testing Rev. 8b.

3.5. Physical design and tuning of TVA

A TVA was designed and manufactured and shown in Fig. 5. This design consists of two brass masses of 64 g at each end of a centrally supported mild steel rod with diameter of 5.5 mm and length of 111 mm. The fixed centre is welded to a hose clamp to allow it to be clamped to the shaft of the electric grass trimmer.

The TVA can be modelled as dual cantilevered mass which can be represented as two discrete system. The rod itself is assumed to be one system (Fig. 5(a)) and the absorber mass at the end of the rod (Fig. 5(b)) is another. Neglecting damping of the TVA system, the natural frequency of the TVA, ω_{cb} can be determined using Dunkerleys approximation (Rajasekaran, 2009):

$$\frac{1}{\omega_{cb}^2} = \frac{1}{\omega_b^2} + \frac{1}{\omega_a^2} \tag{9}$$

The natural frequency of the cantilever beam, ω_b

$$\omega_b = 3.52\sqrt{\frac{EI}{m_b l_b^3}} \tag{10}$$

where the Young's modulus of steel, $E = 200$ GPa, second moment of inertia of the cantilever beam, $I = 1/4\pi r^4$, the mass of cantilever beam, $m_b = \rho_{\text{steel}}\pi r^2 l_b$, r is the radius of cantilever beam, l_b is the length of the cantilever beam and ρ_{steel} is the density of steel.

The natural frequency of cantilever beam with secondary mass m_a attached at the end, ω_a can be rewritten as:

$$\omega_a = \sqrt{\frac{3EI}{m_a l_a^3}} \tag{11}$$

where l_a is the length from the fixed centre to secondary mass.

The TVA is tuned to the operating frequency of electric grass trimmer, 220 Hz as measured in Section 4.1. To tune the resonant frequency of the TVA, the length between brass mass and the fixed centre is adjusted. In order to verify the tuning, spectral analysis was carried out where the results confirmed the natural frequency of the TVA to be 220 Hz.

3.6. Structural modification prediction

Attaching a TVA to the shaft of electric grass trimmer modified its dynamic behaviour and this is predicted using SM procedure as discussed in Section 2. Although FE method is popular and can be used for this purpose, real structural model differs from the FE model due to the difficulty in correctly modelling non-linearities in the structural parameters or boundary conditions (for example the contact between the tubular structure and the plastic housing). Therefore, FRF modification from experimental modal analysis (Section 3.3) is carried with more confidence for SM purpose. This can be directly executed from the LMS Test Lab Modification Prediction software which evaluates the changes in natural frequencies, mode shapes, damping and FRFs of the structural directly from experimental modal analysis data.

A model of the electric grass trimmer was developed and shown in Fig. 6. The modelling was explained earlier in Section 3.3. Each node represents the point of measurement made in the experimental modal analysis. A simulated TVA ($m_t = 0.2$ kg, $k_t = 382151$ N/m, $c_t = 0$ kg/s) was located on the shaft, from points p:10 to p:19. The TVA was tuned to 220 Hz in order to match the operating frequency of the electric grass trimmer. Although the natural frequencies, mode shape and damping can be predicted on each simulated TVA location, this study is only concerned with the predicted FRF at 220 Hz which identified the minimum FRF as the design objective.

3.7. Selection of the TVA location

In this section, the TVA is mounted on the shaft of the electric grass trimmer. The TVA is located at various points along the shaft (L) as shown in Fig. 7 which correspond to points p: 10 to p: 19 in the simulation (Fig. 6). The measurements between intermediate points in Fig. 6 were also taken into account. For each TVA location,

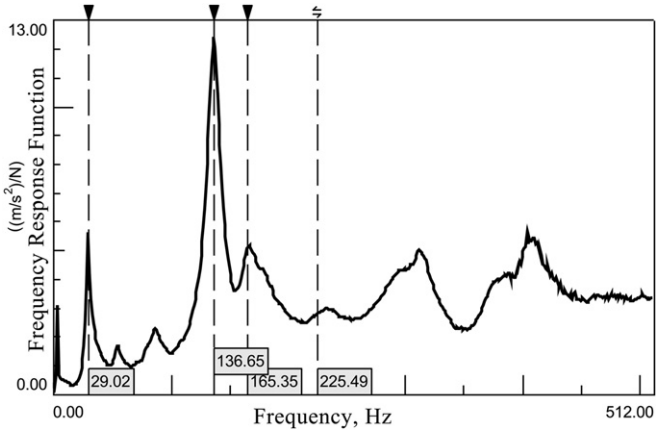

Fig. 9. Summation of FRF curves of electric grass trimmer.

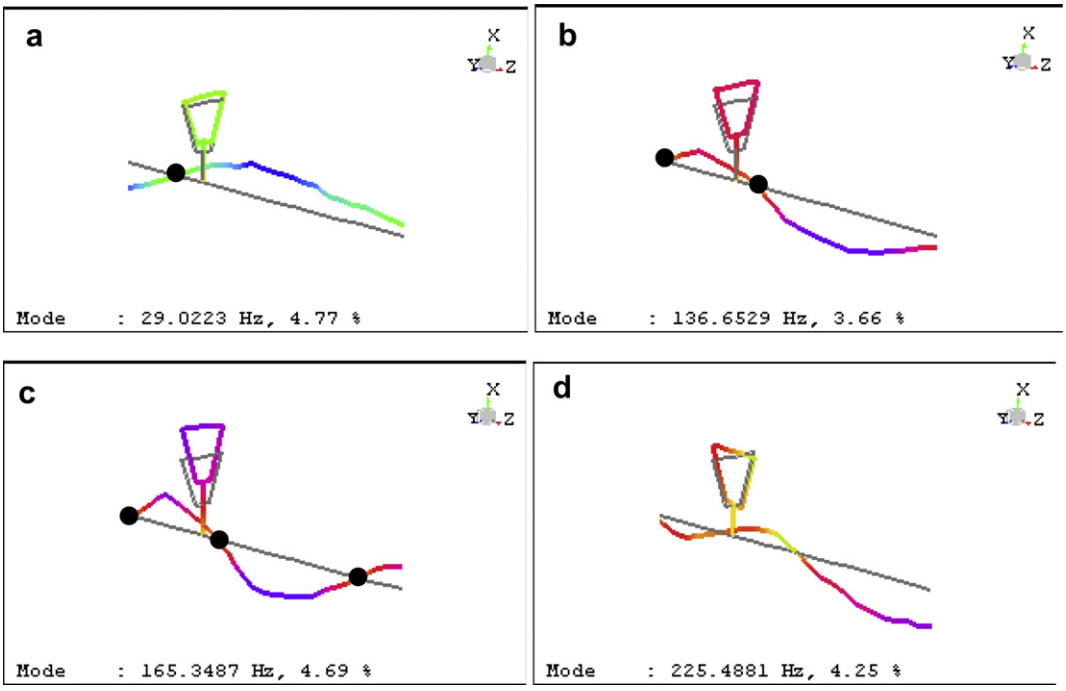

Fig. 10. Mode shape and location of node of electric grass trimmer.

acceleration of the front handle location (corresponding to point *p*: 25 in Fig. 6) is measured. By comparing the measured acceleration, the TVA location which produced the minimum FRF of the handle vibration at 220 Hz is chosen as the optimum location. Field test and subjective evaluation are then carried on the electric grass trimmer with TVA attached at the optimum location.

3.8. Field test and subjective evaluation

Ten representative male operators were chosen for this study and their attributes are summarized in Table 1. All operators were in good physical condition and had some experience in using electric grass trimmer. Ear muffs were provided to all operators during each task for hearing protection.

Before the field test, all the operators were briefed about the objective of the experiments. For measuring HAV, the miniature accelerometer was mounted on the front handle of electric grass trimmer, as near as possible to the point of entry of vibration to the hand (ISO 5349-2, 2001). The three different orientations (X_{h}-, Y_{h}-, Z_{h}- axes) of mounting the accelerometer are based on ISO 5349 standard. The accelerometer was connected to LMS Scadas Mobile, and the data were analyzed using LMS spectral testing software.

Two electric grass trimmers (with and without TVA) were warmed up until stable conditions were reached before the experiment commenced (BS EN ISO 22867, 2008). The operators

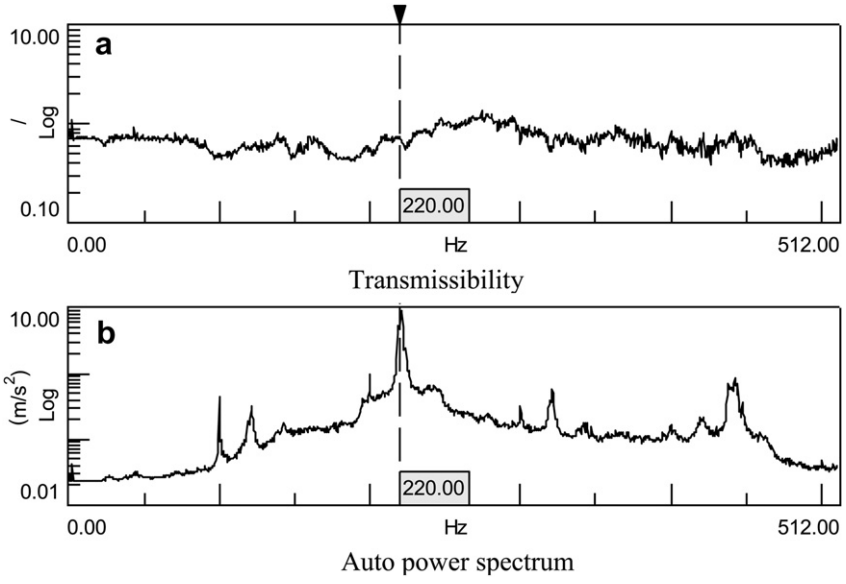

Fig. 11. Transmissibility measurement and auto power spectrum.

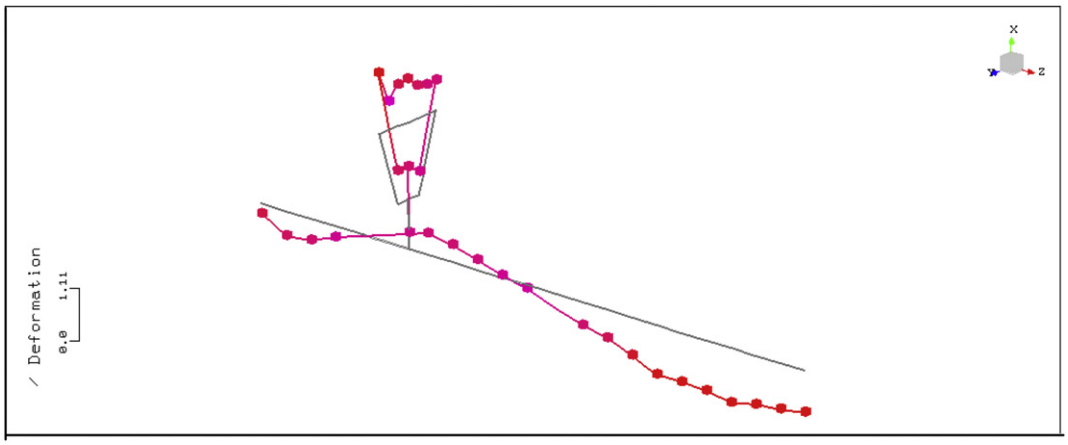

Fig. 12. ODS for electric grass trimmer at operating frequency (220 Hz).

were then requested to operate electric grass trimmers with the different set of grass trimmer and perform two operations, namely no cutting and cutting. For each measurement, the operator was asked to operate the electric grass trimmer at full engine speed of 13200 rpm for 60 s. The stored data were later analyzed for vibration acceleration in rms (a_{hj}) at 1/3rd octave bands centred from 16 to 1000 Hz for each measurement and each axis. For each axis, the overall weighted rms acceleration (a_{hwx},a_{hwy} ,a_{hwz}) was calculated according ISO 5349-2 (2001). From the overall weighted rms acceleration of three axes, vibration total value (a_{hv}) was calculated for each operator. Average of vibration acceleration of the 10 operators was calculated which represented the vibration exposure of electric grass trimmer. The reduction of vibration was calculated by subtracting the averaged vibration total value (a_{hv}) of grass trimmer without TVA from the one with TVA.

After each test, the operators were asked to rate the electric grass trimmer in terms of perception of vibration. The subjective ratings were made using the Borg CR-10 scale (Wos et al., 1988). The CR-10 scale consists of numerical scale from 0 to 10 (0-no vibration, 1-little vibration, 3-moderate vibration, 5-strong vibration, 7-very strong vibration, 10-extreme strong vibration). The operators were asked to report honestly based on what they feel and experienced.

One-way analysis of variance (ANOVA) was performed to test the different level of frequency-weighted rms acceleration of different axis among the electric grass trimmer. The *t*-test was then conducted to calculate the vibration reduction level of the electric grass trimmer with TVA from the one without.

4. Results and discussions

4.1. Vibration analysis of electric grass trimmer

The acceleration spectra of electric grass trimmer measured in $X_{h\text{-}}$, $Y_{h\text{-}}$, and $Z_{h\text{-}}$ axes are illustrated in Fig. 8. Only frequencies in the range of 0–500 Hz are shown. Electric grass trimmer employed in this study had the highest peak in the $Z_{h\text{-}}$ axis at 220 Hz with magnitude of 181.17 m/s^2. Meanwhile for the $X_{h\text{-}}$ and $Y_{h\text{-}}$axes at 220 Hz, the magnitudes of accelerations were 106.46 m/s^2 and 4.74 m/s^2 respectively. The torsional vibration of the telescopic tubular structure manifests itself as acceleration in the $Y_{h\text{-}}$ axis (a_y = radius of the circular path × angular acceleration) and has the lowest acceleration. The dominant frequency of 220 Hz correlated with the speed of the cutter head of 13200 rpm. The handle vibration spectra also exhibits peaks at higher frequencies, near 325 Hz, 450 Hz, but with much lower amplitude. This clearly showed that the peaks due to cutter head rotational speed are well separated from the others. This observation suggests the possibility of using a TVA tuned to the electric grass trimmer's dominant operating frequency, to reduce the vibration level at the handle.

4.2. Experimental modal analysis of electric grass trimmer

Detection of vibration modes can be identified from measured FRF data during experimental modal analysis. Fig. 9 presents the summation of FRFs since the identification of vibration modes is preferable based on several FRF curves (He and Fu, 2001). This is to ensure that vibration modes become distinguished in the total FRF plot. Obviously from Fig. 9, it contains few peaks. However, not every peak of an FRF is necessary a real mode and some modes may be invisible in the frequency range (He and Fu, 2001). The best way to visualize vibration modes is by animating the mode shapes.

Fig. 10 illustrated the corresponding mode shapes. The first bending mode of electric grass is at 29 Hz (corresponding to peak at 29 Hz in Fig. 9) which exhibits a node between *p*:4 and *p*: 20 (handle location). The second bending mode occurred at 136 Hz and has two nodes located between *p*:1 and *p*:2 and between *p*:5 and *p*:6. Meanwhile at 165 Hz the third bending mode occurs with three nodes at *p*:1-p:2, *p*:5-*p*:6 and *p*:14-*p*:15. What is evident from these frequencies is the mode shape at 225 Hz with two nodes at

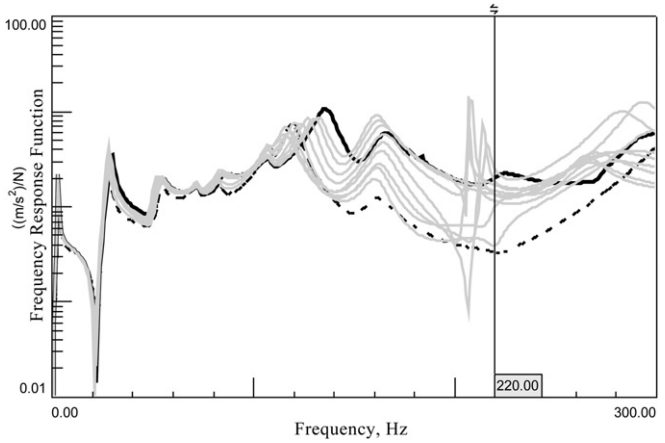

Fig. 13. FRF modification on handle response with different TVA location (—: measured FRF (without TVA); —: predicted FRFs; ---: predicted FRF with minimum response at 220 Hz).

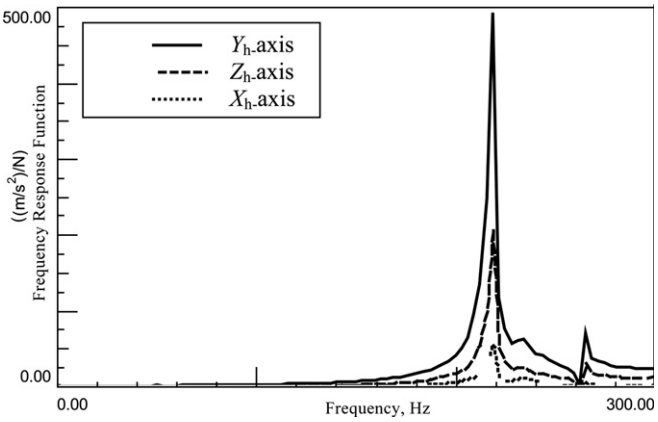

Fig. 14. FRFs of TVA.

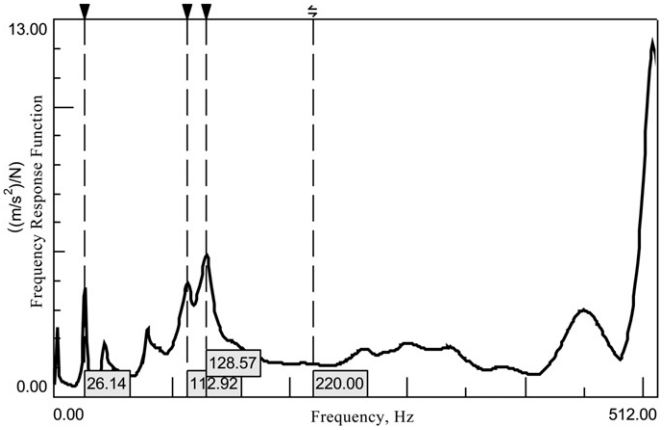

Fig. 16. Summation of FRF curves of electric grass trimmer with TVA attached at optimum location.

p:5-*p*:6 and *p*:9-*p*:10. This mode is very close to the excitation frequency (220 Hz). This may have contributed to the generally large amplitude of handle vibration at the operating frequency.

4.3. ODS analysis of electric grass trimmer

ODS analysis of the electric grass trimmer was carried out on in order to determine the vibration shape at the operating frequency of 220 Hz. This is important in order to detect whether the installation of the TVA has shifted the location of the node closer or further away from the handle since any substructure located at the node will influence an almost zero vibration.

The transmissibility obtained from ODS analysis is shown in Fig. 11(a). It is noted that the peaks in the magnitude of the transmissibility function do not represent the resonances peak in the auto power spectrum (Fig. 11(b)). This property of transmissibility differs from those ODS frequency domain measurements (Christof et al., 2010; Devriendt and Guillaume, 2008; Schwarz and Richardson, 1999). Instead, the transmissibility function has no peak in the frequency range where a resonance peak occurs.

The ODS for the electric grass trimmer at the operating frequency of 220 Hz is shown in Fig. 12. The ODS indicated that the handle vibration suffers from two basic problems. Firstly, the operating frequency of 220 Hz is close to the resonant frequency of electric grass trimmer (mode at 225 Hz, Fig. 10 (d)). Secondly, the location of the handle is very close to the anti-node of the shaft, which is clearly shown in Fig. 12. From these two points, vibration attenuation can be achieved by changing the natural frequency or by altering the location of the node to be close to or at the point of the handle itself.

4.4. Predicted FRF of handle grip response

Due to physical constraint, the TVA can only be attached at points *p*:10 to *p*:19 along the tubular structure. The effect of attaching the TVA along these locations on the handle grip response (*p*:25) has been studied. The predicted responses at handle grip location (at *p*:25) varied with the different attachment points of the TVA are shown in Fig. 13. The measured FRF handle

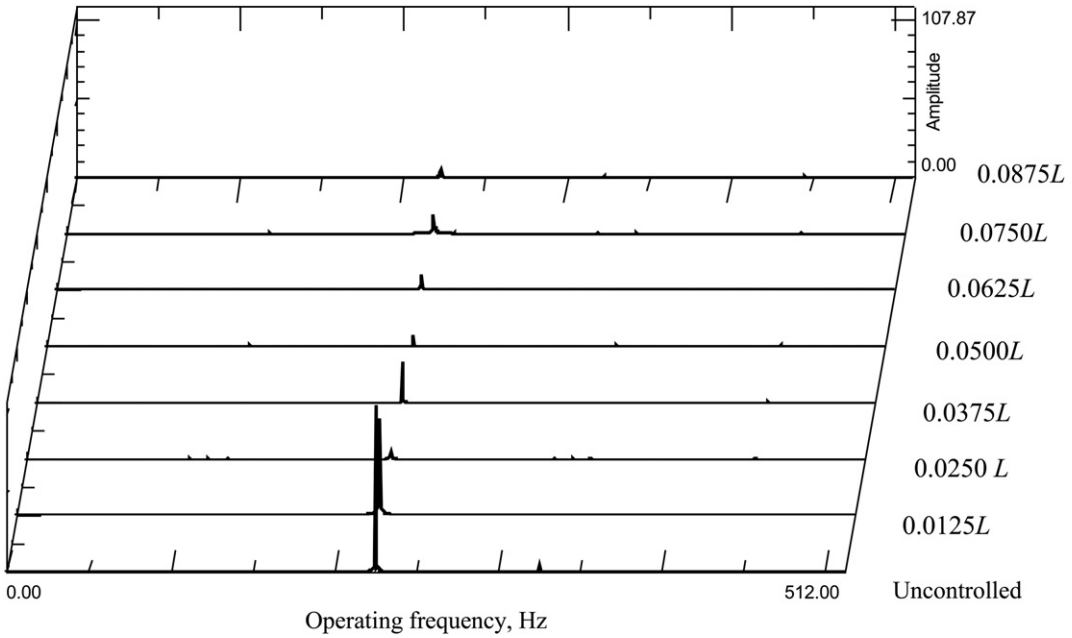

Fig. 15. Vibration amplitude of the handle in X_h- axis with TVA attached at a different location.

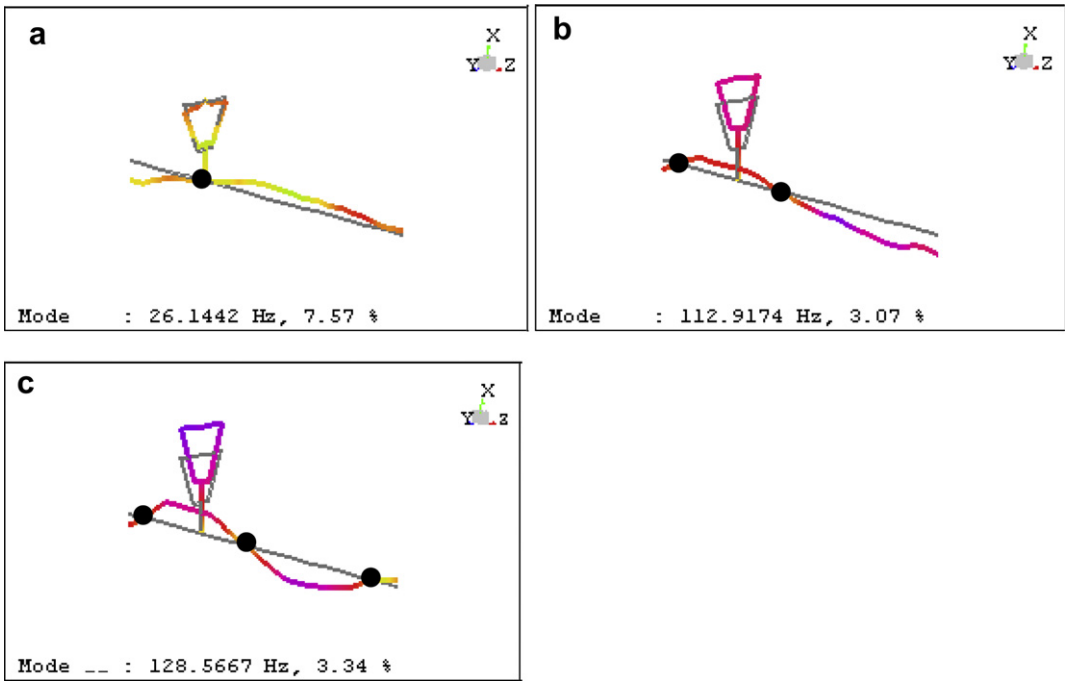

Fig. 17. Mode shape and location of node of electric grass trimmer with TVA attached at optimum location.

response without TVA is shown in Fig. 13 and has the value of 2.01 $(m/s^{-2})/N$. With the simulated TVA attached at each point, the predicted FRF response showed the values in the range of 0.33–1.86 $(m/s^{-2})/N$. The best location is predicated at point p:10 which give the lowest FRF values of $0.33(m/s^{-2})/N$.

4.5. Tuning of TVA

The plot of the FRFs obtained from the tuning experiment is shown in Fig. 14. For the masses located at a distance of 28 mm (as calculated from Section 3.5) from the fixed centre of TVA showed that natural frequency of the TVA was measured at 220 Hz. Y_h- axis has the highest peak followed by the Z_h- axis and the X_h- axis. This result also showed that the modal damping ratio of the TVA is 0.39%. This indicated that the TVA is lightly damped and can be defined as an undamped TVA.

4.6. Optimum TVA location

A series of experiment was carried out to investigate the effect of varying the position of TVA along the tubular structure ($L = 40$ cm). The resulting acceleration of the handle varied with the TVA location. The experimentally obtained results agreed that the optimum location of attachment location was near point, p: 10 as predicted in Section 4.4. Hence, only first seven cases were displayed, as illustrated in waterfall diagram (Fig. 15), namely0.0125L, 0.025L, 0.0375L, 0.05L, 0.0625L, 0.075L and 0.0875L which correspond to the points between p:10 and p:11 in the SM simulation. The figure shows the acceleration at 220 Hz for grass trimmer without TVA is 106.46 m/s^2. The experiments were repeated to evaluate the response for the different attachment positions. In these cases, the TVA produced different reduction of vibration acceleration. For this frequency (220 Hz), position 0.025L clearly appeared to be optimum with reduction of 101.62 m/s^2 (about 95%)

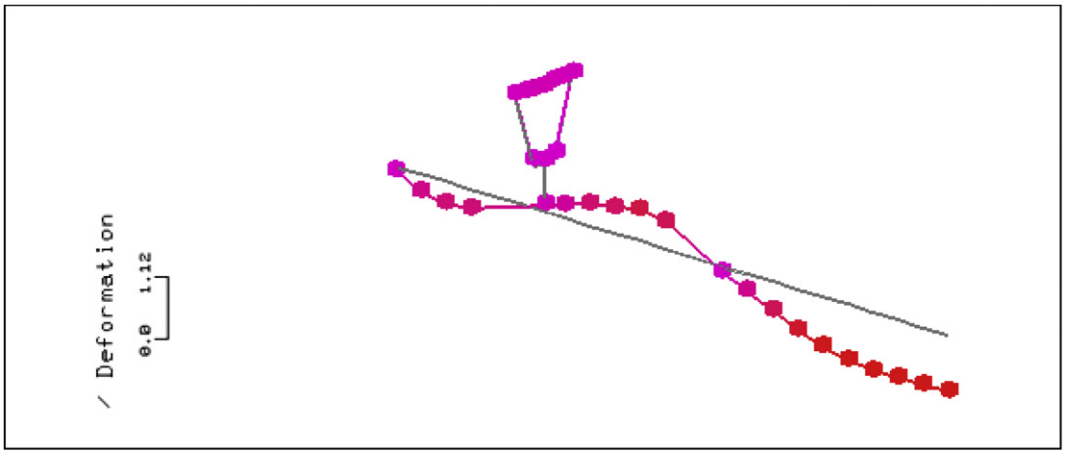

Fig. 18. ODS for electric grass trimmer with TVA at operating frequency (118 Hz).

of handle acceleration level. Reduction of 44.02 m/s^2, 80.23 m/s^2, 98.66 m/s^2, 96.54 m/s^2, 94.21 m/s^2, 100.56 m/s^2 were achieved, when the TVA was located at positions 0.0125*L*, 0.0375*L*, 0.05*L*, 0.0625*L*, 0.075*L* and 0.0875*L* respectively. It has therefore been demonstrated that the optimum location of the TVA can be obtained within the practical length of the tubular structure.

4.7. Experimental modal analysis and ODS of electric grass trimmer after instalment of TVA

Experimental modal analysis was carried out for the electric grass trimmer with the TVA mounted on the shaft at the optimum location (0.025*L*) identified from the SM simulation. Fig. 16 shows

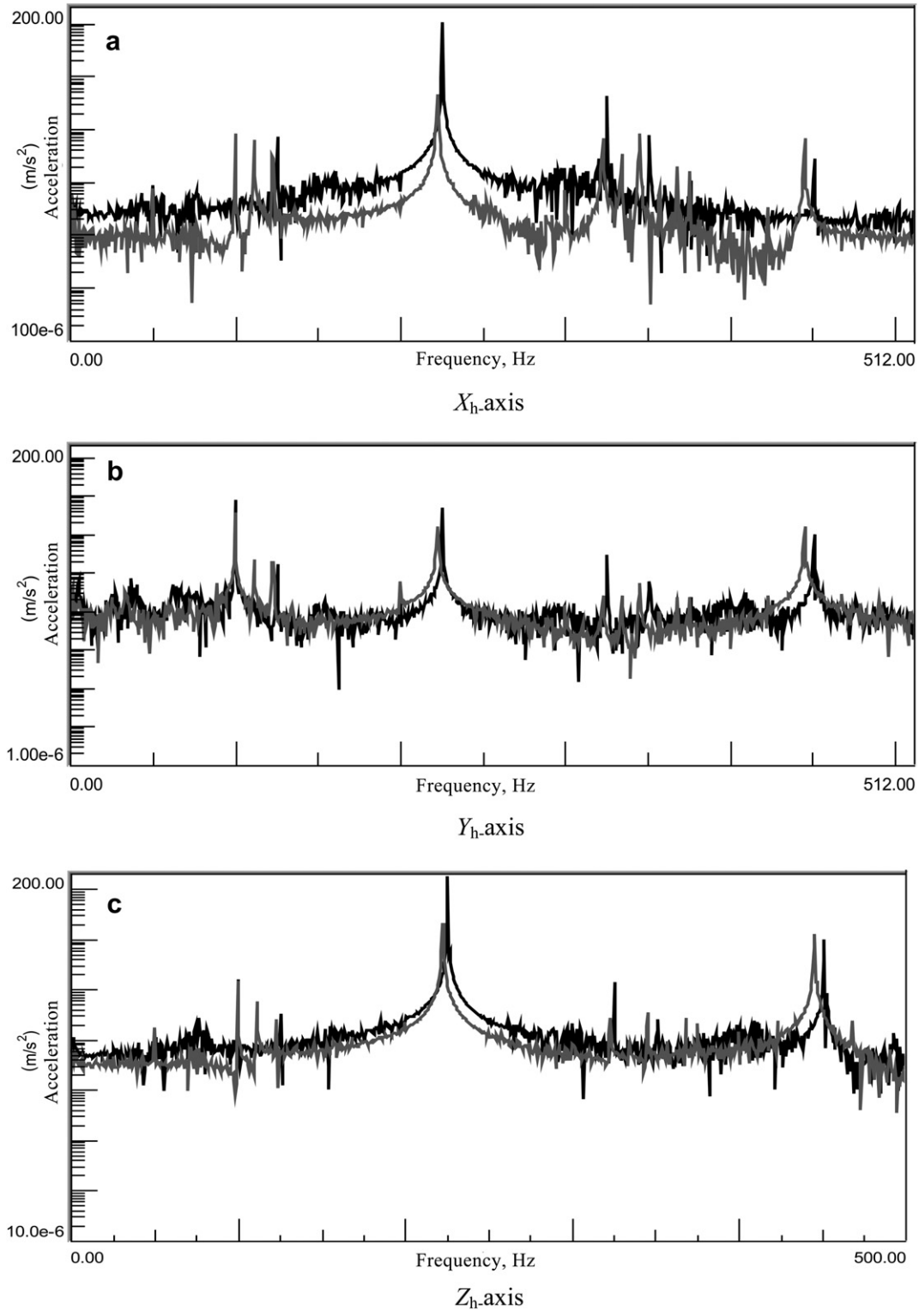

Fig. 19. Acceleration spectra of electric grass trimmer with and without TVA (—:without TVA; —: with TVA attached at optimum location).

three resonance peaks in the frequency range of 20–250 Hz, but there were none between 200 and 250 Hz. This indicated that the presence of TVA produces lower FRF than the original FRF (Fig. 9) in the range of excitation frequencies. The corresponding mode shape of these resonances (Fig. 17) was similar with the original machine (Fig. 10). However, these mode shapes occurred at lower frequencies due to the additional mass from the TVA. Although the new modified electric grass trimmer created new resonant modes, especially at 450 Hz and 508 Hz, these are outside the operating frequency range of the electric grass trimmer.

The ODS analysis for the electric grass trimmer with TVA was also carried out, and the deflection shape is displayed in Fig. 18. In order to make a direct comparison of the effect of TVA, deformation scale in Fig. 18 is set to be the same with that in Fig. 12. The result from this investigation showed that the TVA has successfully reduced the vibration of the handle. It may be interest to note that the node is now shifted near the handle location. This is a proof that it is practically possible to make the node coincide with the handle location, as numerically proven in the literatures (Cha and Pierre, 1999; Cha, 2002; Cha, 2005; Cha and Ren, 2006; Cha and Zhou, 2006; Cha and Chan, 2009; Foda and Bassam, 2006).

4.8. Effectiveness of TVA in optimum location

4.8.1. Acceleration spectra

The acceleration spectra plots are shown in Fig. 19 to illustrate the effectiveness of the TVA at the optimum location (0.025L) in $X_{h\text{-}}$, $Y_{h\text{-}}$, $Z_{h\text{-}}$ axes. The black line represents the acceleration level of handle without TVA, and the grey line represents the acceleration response of handle with TVA. These figures indicated that the TVA can selectively reduce acceleration level within the frequency range of 130 Hz–320 Hz in the $X_{h\text{-}}$ and $Z_{h\text{-}}$ axes. During this measurement, reduction in the supply voltage from the nominal 240 V has resulted in the slight reduction the operating frequency, from 220 Hz to 218 Hz Fig. 19(a) demonstrates that the TVA can effectively reduce the peak acceleration from 106.46 m/s^2 to 4.83 m/s^2 in the $X_{h\text{-}}$ axis. The acceleration of the handle was reduced by 95% while the mass was only increased by 7%. The dynamic force was reduced by 277.5 N. This highlighted the effectiveness of the dynamic force reduction with the use of TVA. However, as can been seen in Fig. 19(b), the TVA has very little effect in the $Y_{h\text{-}}$ axis. Although the amplitude increased in the frequency range of 190–220 Hz, the effect is not significant since $Y_{h\text{-}}$ axis contributes the least to the vibration total value. Fig. 19(c) shows that the TVA also reduces the acceleration level in $Z_{h\text{-}}$ axis.

4.8.2. Frequency-weighted rms acceleration and vibration total value

Table 2 illustrates the frequency-weighted rms acceleration ($X_{h\text{-}}$, $Y_{h\text{-}}$ and $Z_{h\text{-}}$ axes) and vibration total value for electric grass trimmer with and without TVA in the no cutting and cutting conditions. It shows that frequency-weighted rms acceleration for both cases increase when cutting operation is carried out. For example in the case without TVA, frequency-weighted rms acceleration increase from 2.38 m/s^2 to 2.83 m/s^2 in the $X_{h\text{-}}$ axis, 0.75 m/s^2 to 0.93 m/s^2 in the $Y_{h\text{-}}$ axis, 3.24 m/s^2 to 3.37 m/s^2 in the $Z_{h\text{-}}$ axis and 4.11 m/s^2 to 4.54 m/s^2 for vibration total value. In the same condition of electric grass trimmer with TVA, the frequency-weighted rms acceleration of 0.78–1.30 m/s^2 during no cutting was increased to 0.79–1.48 m/s^2 during the cutting operation.

Table 2
Frequency-weighted rms acceleration and standard deviation.

Condition	TVA	$X_{h\text{-}}$ axis (m/s^2)	$Y_{h\text{-}}$ axis (m/s^2)	$Z_{h\text{-}}$ axis (m/s^2)	Vibration total value (a_{hv})(m/s^2)
No cutting	without	2.38 ± 0.14	0.75 ± 0.12	3.24 ± 0.62	4.11 ± 0.46
	with	0.78 ± 0.13	0.83 ± 0.16	0.59 ± 0.10	1.30 ± 0.16
Cutting	without	2.83 ± 0.36	0.93 ± 0.18	3.37 ± 1.07	4.54 ± 0.93
	with	0.79 ± 0.20	1.12 ± 0.24	0.53 ± 0.10	1.48 ± 0.28

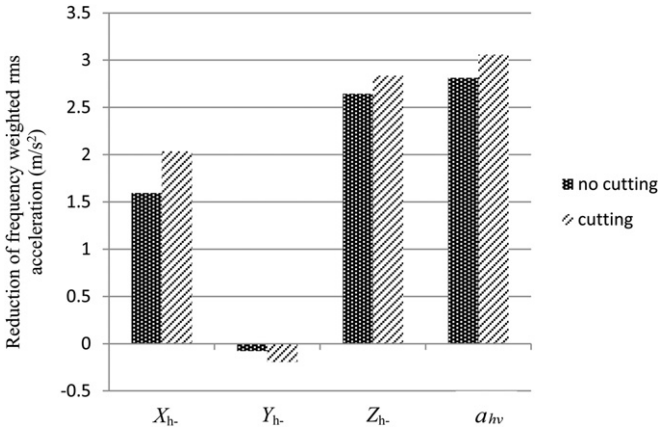

Fig. 20. Effect of TVA on reduction of frequency-weighted rms acceleration at various axes and vibration total value.

4.8.3. Reduction of vibration

The reduction of vibration was calculated by subtracting the vibration acceleration of the electric grass trimmer when operating without the TVA from the condition with the TVA installed. Fig. 20 illustrates the effect of TVA on the average frequency-weighted rms acceleration in the $X_{h\text{-}}$, $Y_{h\text{-}}$, $Z_{h\text{-}}$ axes and vibration total value. The average reduction of frequency-weighted rms acceleration was 1.59 m/s^2, 2.64 m/s^2 and 2.81 m/s^2 at $X_{h\text{-}}$, $Z_{h\text{-}}$, and vibration total value respectively for the no cutting condition. Thus the reduction of vibration in the $X_{h\text{-}}$ axis was 67%, in the $Z_{h\text{-}}$ axis was 82% and 68% for vibration total value. The reduction of the frequency-weighted rms acceleration in the different axis during the cutting operation is also shown in the same figure. It is observed that the reduction of vibration was highest in the $Z_{h\text{-}}$ axis, which is 2.84 m/s^2 (84%). Whereas reduction of 2.04 m/s^2 (72%) and 3.06 m/s^2 (67%) were observed in the $X_{h\text{-}}$ axis and vibration total value. However, amplification of frequency-weighted rms accelerations was found in the $Y_{h\text{-}}$ axis, 19% for the no cutting condition and 21% for cutting operation.

The performance of TVA in both no cutting and cutting operations is further shown in Table 3. Introducing TVA to the electric grass trimmer significantly ($p < 0.01$) reduce the HAV in the $X_{h\text{-}}$, $Z_{h\text{-}}$ axes and vibration total value for both cutting and no cutting operation. Although there were amplification of vibration in the $Y_{h\text{-}}$ axis, the amplifications were insignificant since the p values were greater than 0.01.

Table 3
The t-test values for the reduction of frequency-weighted acceleration in different conditions.

Condition	Paired differences	t-values			
		$X_{h\text{-}}$ axis	$Y_{h\text{-}}$ axis	$Z_{h\text{-}}$ axis	Vibration total value (a_{hv})
No cutting	Without TVA − with TVA	27.415*	−1.299	12.886*	16.921*
Cutting	Without TVA − with TVA	15.157*	−1.513	8.014*	9.471*

*Significant ($p < 0.01$).

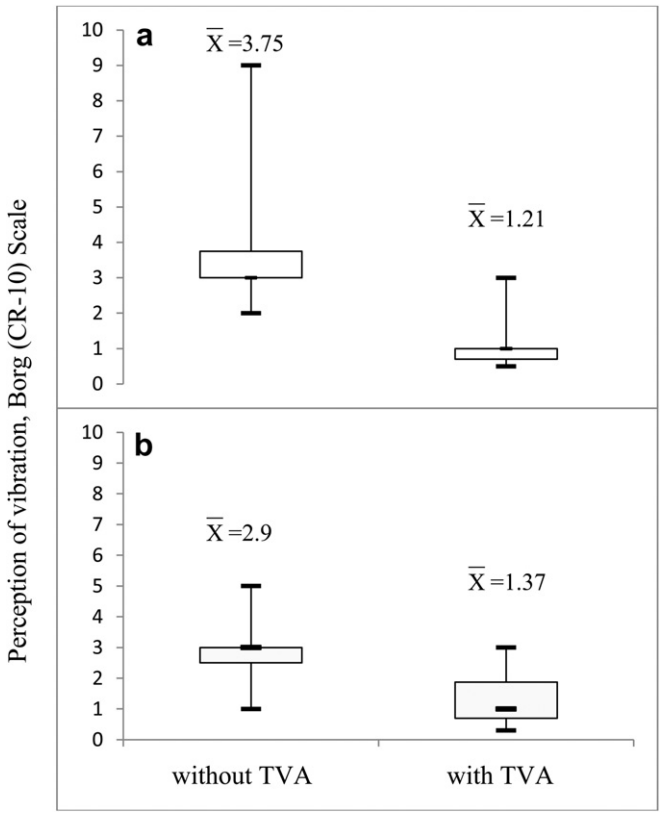

Fig. 21. Perception of vibration based on Borg scale: (a) no cutting, (b) cutting.

4.8.4. Subjective evaluation: rating of vibration perception

The box plot in Fig. 21 shows the rating of vibration perception in the Borg (CR-10) scale during no cutting and cutting operations. For both conditions, the electric grass trimmer with the instalment of TVA received better rating (lower value in Borg scale) for the perception of vibration. It can be seen that the mean vibration perception during no cutting operation was 3.75. The presence of TVA reduced the vibration to the level of 1.21 (68%). Similarly, during the cutting operation, the mean vibration perception was 2.9. The vibration was reduced to 1.37 (53%) with the controlled electric grass trimmer. The results proved that the electric grass trimmer with TVA received better overall vibration perception than without.

5. Conclusion

The goal of this work was to develop a vibration suppression strategy that could effectively reduce handle vibration of an electric grass trimmer. A TVA was simulated and designed to be attached to the shaft of electric grass trimmer. The TVA was tuned to the operating frequency (220 Hz) of electric grass trimmer to attenuate handle vibration. An optimum absorber location ($0.025L$) was also identified both analytically and experimentally. The electric grass trimmer with the TVA installed in the optimum location is effective in reducing acceleration level of vibration. The TVA was found to have best performance with 95% reduction on the acceleration level in the $X_{\text{h-}}$ axis. The results from experimental modal analysis and ODS showed that the presence of TVA has successfully reduced the large vibrations of the handle where the node was shifted nearer to the handle location. Both the measured overall weighted rms acceleration and subjective evaluation results obtained from the field tests were consistently indicating that the electric grass trimmer with TVA has lower handle vibration than without.

Acknowledgements

The authors would like to express their gratitude to all the operators who have participated in this research. The support of the Universiti Sains Malaysia Fellowship is fully acknowledged. This research work was funded by the Ministry of Science, Technology and Innovation through the e-science fund account No. 6013360. The assistance of Encik Baharum bin Awang and Encik Wan Amri are greatly acknowledged.

Appendix. Nomenclature

DOF	degrees-of-freedom
FE	finite-element
FRF	frequency response function
FRFs	frequency response functions
HAV	hand-arm vibration
HAVS	hand-arm vibration syndrome
MDOF	multiple-degrees-of freedom
ODS	operational deflection shape
rms	root mean square
SDOF	single-degree-of-freedom
SM	structural modification
TVA	tuned vibration absorber
C	damping
$\tilde{\text{C}}$	new damping after structural modification
c_t	damping of TVA
K	stiffness
$\tilde{\text{K}}$	new stiffness after structural modification
k_t	stiffness of TVA
M	mass
$\tilde{\text{M}}$	new mass after structural modification
m_t	mass of TVA
$\{x\}$	displacement vector
$\{f\}$	force vector
Φ	Eigenvector
Λ	Eigenvalue
[]	matrix
{}	vector
ΔM	modified mass
ΔC	modified damping
ΔK	modified stiffness
$[s(\omega)]$	dynamic stiffness matrix
$[H(\omega)]$	FRF matrix
$[\Delta s(\omega)]$	modified dynamic stiffness matrix
$[H_m(\omega)]$	modified FRF matrix
a_{hv}	vibration total value
a_{hwx}	weighted rms acceleration in $X_{\text{h-}}$ axis
a_{hwy}	weighted rms acceleration in $Y_{\text{h-}}$ axis
a_{hwz}	weighted rms acceleration in $Z_{\text{h-}}$ axis
ω_{cb}	natural frequency of the TVA
ω_b	natural frequency of the cantilever beam
ω_a	natural frequency of cantilever beam with secondary mass m_a
E	Young's modulus
I	second moment of inertia of the beam
m_b	mass of the beam
ρ_{steel}	density of steel
r	radius of beam
l_b	length of beam
m_a	secondary mass
l_a	length from the fixed centre to secondary mass

References

Asami, T., Nishihara, O., Baz, M.A., 2002. Analytical solutions to H∞ and H_2 optimization of dynamic vibration absorbers attached to damped linear systems. Journal of Vibration and Acoustics 124, 284–295.

BS EN ISO 11806, 2008. Agricultural and Forestry Machinery. Portable Hand-held Combustion Engine Driven Brush Cutters and Grass Trimmers Safety. International Standard Organization, Geneva.

BS EN ISO 22867, 2008. Forestry Machinery. Vibration Test Code for Portable Hand-held Machines with Internal Combustion Engine. Vibration at the Handles. International Standard Organization, Geneva.

Brennan, M.J., 2000. Actuators for active control-tunable resonant devices. Applied Mechanics and Engineering 5 (1), 63–74.

Brennan, M.J., Dayou, J., 2000. Global control of vibration using a tunable vibration neutralizer. Journal of Sound and Vibration 232 (3), 585–600.

Brown, A.P., 1990. The effects of anti-vibration gloves on vibration induced disorders: a case study. Journal of Hand Therapy 3, 94–100.

Bylund, S., 2004. Hand-arm vibration and working women: consequences and affecting factors. Umeå University. (Thesis).

Cha, P., 2002. Specifying nodes at multiple locations for any normal mode of a linear elastic structure. Journal of Sound and Vibration 250, 923–934.

Cha, P., 2005. Enforcing nodes at required locations in a harmonically excited structure using simple oscillators. Journal of Sound and Vibration 279, 799–816.

Cha, P., Chan, M., 2009. Mitigating vibration along an arbitrarily supported elastic structure using multiple two-degree-of-freedom oscillators. Journal of Vibration and Acoustics 131 031008.

Cha, P., Pierre, C., 1999. Imposing nodes to the normal modes of a linear elastic structure. Journal of Sound and Vibration 219, 669–687.

Cha, P., Ren, G., 2006. Inverse problem of imposing nodes to suppress vibration for a structure subjected to multiple harmonic excitations. Journal of Sound and Vibration 290, 425–447.

Cha, P., Zhou, X., 2006. Imposing points of zero displacements and zero slopes along any linear structure during harmonic excitations. Journal of Sound and Vibration 297, 55–71.

Cheung, Y.L., Wong, W.O., 2008. Isolation of bending vibration in a beam structure with a translational vibration absorber and a rotational vibration absorber. Journal of Vibration and Control 14 (8), 1231–1246.

Christof, D., Gunther, S., Gert, D.S., Patrick, G., 2010. From operating deflection shapes towards mode shapes using transmissibility measurements. Mechanical Systems and Signal Processing 24 (3), 665–677.

Dayou, J., 2006. Fixed-points theory for global vibration control using vibration neutralizer. Journal of Sound and Vibration 292, 765–776.

Dayou, J., Brennan, M.J., 2002. Global control of structural vibration using multiple-tuned tunable vibration neutralizers. Journal of Sound and Vibration 258 (2), 345–357.

Den Hartog, J.P., 1956. Mechanical Vibrations, fourth ed.. McGraw-. Hill Book Co., New York.

Devriendt, C., Guillaume, P., 2008. Identification of modal parameters from transmissibility measurements. Journal of Sound and Vibration 314, 343–356.

Dong, R.G., McDowell, T.W., Welcome, D.E., Smutz, W.P., Schopper, A.W., Warren, C., Wu, J.Z., Rakheja, S., 2003. On-the-hand measurement methods for assessing effectiveness of anti-vibration gloves. International Journal of Industrial Ergonomics 32, 283–298.

Esmailzadeh, E., Jalili, N., 1998. Optimum design of vibration absorbers for structurally damped Timoshenko beams. Journal of Vibration and Acoustics 120, 833–841.

Ewins, D.J., 1984. Modal Testing: Theory and Practical. John Wiley & Sons INC, London.

Fasana, A., Giorcelli, E., 2010. A vibration absorber for motorcycle handles. Meccanica 45, 79–88.

Foda, M.A., Bassam, B.A., 2006. Vibration confinement in a general beam structure during harmonic excitations. Journal of Sound and Vibration 295 (3–5), 491–517.

Golysheva, E.V., Babitsky, V.I., Veprik, A.M., 2004. Vibration protection for an operator of a hand-held percussion machine. Journal of Sound and Vibration 274, 351–367.

Gurram, R., Rakheja, S., J. Gouw, G., 1994. Vibration transmission characteristics of the human hand-arm and gloves. International Journal of Industrial Ergonomics 13, 217–234.

He, J., Fu, Z., 2001. Modal Analysis. Butterworth-Heinemann.

International Organisation of Standardisation ISO 5349-1, 2001. Mechanical Vibration- Measurement and Evaluation of Human Exposure to Hand-transmitted Vibration. Part-1: General Requirements.

International Organisation of Standardisation ISO 5349-2, 2001. Mechanical Vibration-measurement and Evaluation of Human Exposure to Hand-transmitted Vibration. Part -2: Practical Guidance for Measurement at the Workplace.

Jang, S.J., Choi, Y.J., 2007. Geometrical design method of multi-degree-of-freedom dynamic vibration absorbers. Journal of Sound and Vibration 303 (1–2), 343–356.

Jimin, He, 2001. Structural Modification. The Royal Society, 359, pp. 187–204.

Kadam, R., 2006. Vibration characterization and numerical modeling of a pneumatic impact hammer. Master Thesis. Virginia Polytechnic Institute and State University.

Kidner, M.R.F., Brennan, M.J., 2002. Variable stiffness of a beam-like neutralizer under fuzzy logic control. Transactions of the ASME, Journal of Vibration and Acoustics 124, 90–99.

Lee, E.C., Nian, C.Y., Tarng, Y.S., 2001. Design of a dynamic vibration absorber against vibrations in turning operations. Journal of Materials Processing Technology 108, 278–285.

Mallick, Z., 2008. Optimization of operating parameters for a back-pack type grass trimmer. International Journal of Industrial Ergonomics 38 (1), 101–110.

Mallick, Z., 2010. Optimization of operating parameters for a back-pack type grass machine. Applied Ergonomics 41 (2), 260–265.

Mansfield, N., 2005. Human Response to Vibration. CRC, New York.

Muralidhar, A., Bishu, R., Hallbeck, M., 1999. The development and evaluation of an ergonomic glove. Applied Ergonomics 30, 555–563.

Ormondroyd, J., Den Hartog, J.P., 1928. The theory of the dynamic vibration absorber. Transactions of the American Society of Mechanical Engineers 50, A9–A22.

Ozer, M.B., Royston, T.J., 2005. Extending Den Hartog's vibration absorber technique to multi-degree-of-freedom systems. Journal of Vibration and Acoustics 127, 341–350.

Petit, F., Loccufier, M., Aeyels, D., 2009. On the attachment location of dynamic vibration absorbers. Journal of Vibration and Acoustics 131, 034501.

Rajasekaran, S., 2009. Structural Dynamics of Earthquake Engineering. CRC Press LLC, Woodhead Publishing Limited, Oxford, Cambridge, New Delhi.

Rakheja, S., Dong, R., Welcome, D., Schopper, A.W., 2002. Estimation of tool-specific isolation performance of antivibration gloves. International Journal of Industrial Ergonomics 30, 71–87.

Rao, S.S., 2004. Mechanical Vibrations, fourth ed. Prentice Hall, New Jersey, USA.

Ren, M.Z., 2001. A variant design of the dynamic vibration absorber. Journal of Sound and Vibration 245, 762–770.

Richardon, M., 1997. . Is it a mode shape or an operating deflection shape? Sound and Vibration Magazine, 1–11. 30th Anniversary. Issue March 1997.

Sam, B., Kathirvel, K., 2006. Vibration characteristics of walking and riding type power tillers. Biosystems Engineering 95, 517–528.

Schwarz, B.J., Richardson, M.H., 1999. Introduction to Operating Deflection Shapes. CSI Reliability, Orlando, FL.

Sestieri, A., 2000. Structural dynamic modification. Sadhana 25 (3), 247–259.

Strydom, J.P.D., Heyns, P.S., van Niekerk, J.L., 2002. Development of a vibration-absorbing handle for rock drills. The Journal of the South African Institute of Mining and Metallurgy, 167–172.

Tewari, V.K., Dewangan, K.N., 2009. Effect of vibration isolators in reduction of work stress during field operation of hand tractor. Biosystems Engineering 103, 146–158.

Thompson, D.J., 2007. A continuous damped vibration absorber to reduce broadband wave propagation in beams. Journal of Sound and Vibration 311, 824–842.

Tudor, A.W., 1996. Hand-arm vibration: product design principles. Journal of Safety Research 27, 157–162.

(40 CFR part 1054) US Environmental Protection Agency, 2010. Phase 3 Exhaust Emission Standards [Online] Available from World Wide Web. http://www.epa.gov/otaq/equip-ld.htm#regs.

Voss, P., 1996. Protection from hand-arm vibration by the use of gloves: possibility or fraud. Proceedings of the Internoise 96 Conference, Liverpool, UK, vol. 4, 1665–1669.

Wimer, B., McDowell, T.W., Xu, X.S., Welcome, D.E., Warren, C., Dong, R.G., 2010. Effects of gloves on the total grip strength applied to cylindrical handles. International Journal of Industrial Ergonomics 40, 574–583.

Wong, W.O., Cheung, Y.L., 2008. Optimal design of a damped vibration absorber for vibration control of structure excited by ground motion. Engineering Structures 30, 282–286.

Wong, W., Tang, S., Cheung, Y., Cheng, L., 2007. Design of a dynamic vibration absorber for vibration isolation of beams under point or distributed loading. Journal of Sound and Vibration 301, 898–908.

Wos, H., Marek, T., Noworol, C., Borg, G., 1988. The reliability of self-ratings based on Borg's scale for hand-arm vibrations of short duration (Part II). International Journal of Industrial Ergonomics 2, 151–156.

Zuo, L., Nayfeh, S.A., 2004. Minmax optimization of multi-degree-of-freedom tuned-mass dampers. Journal of Sound and Vibration 272, 893–908.